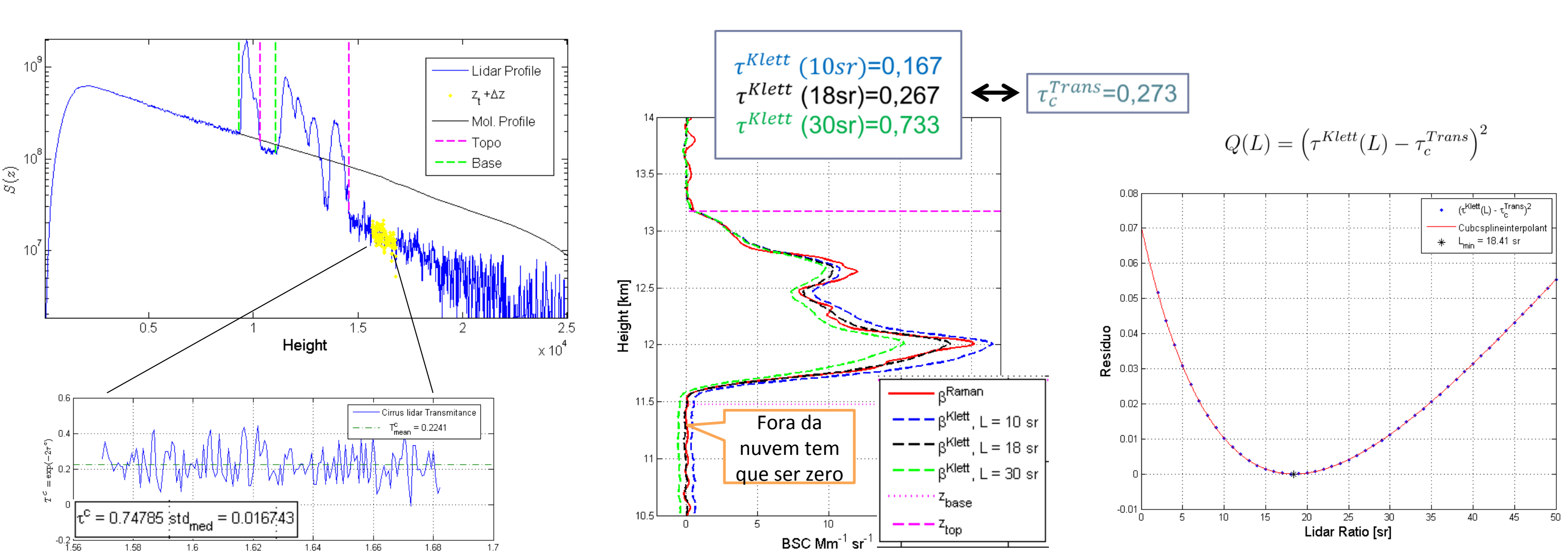
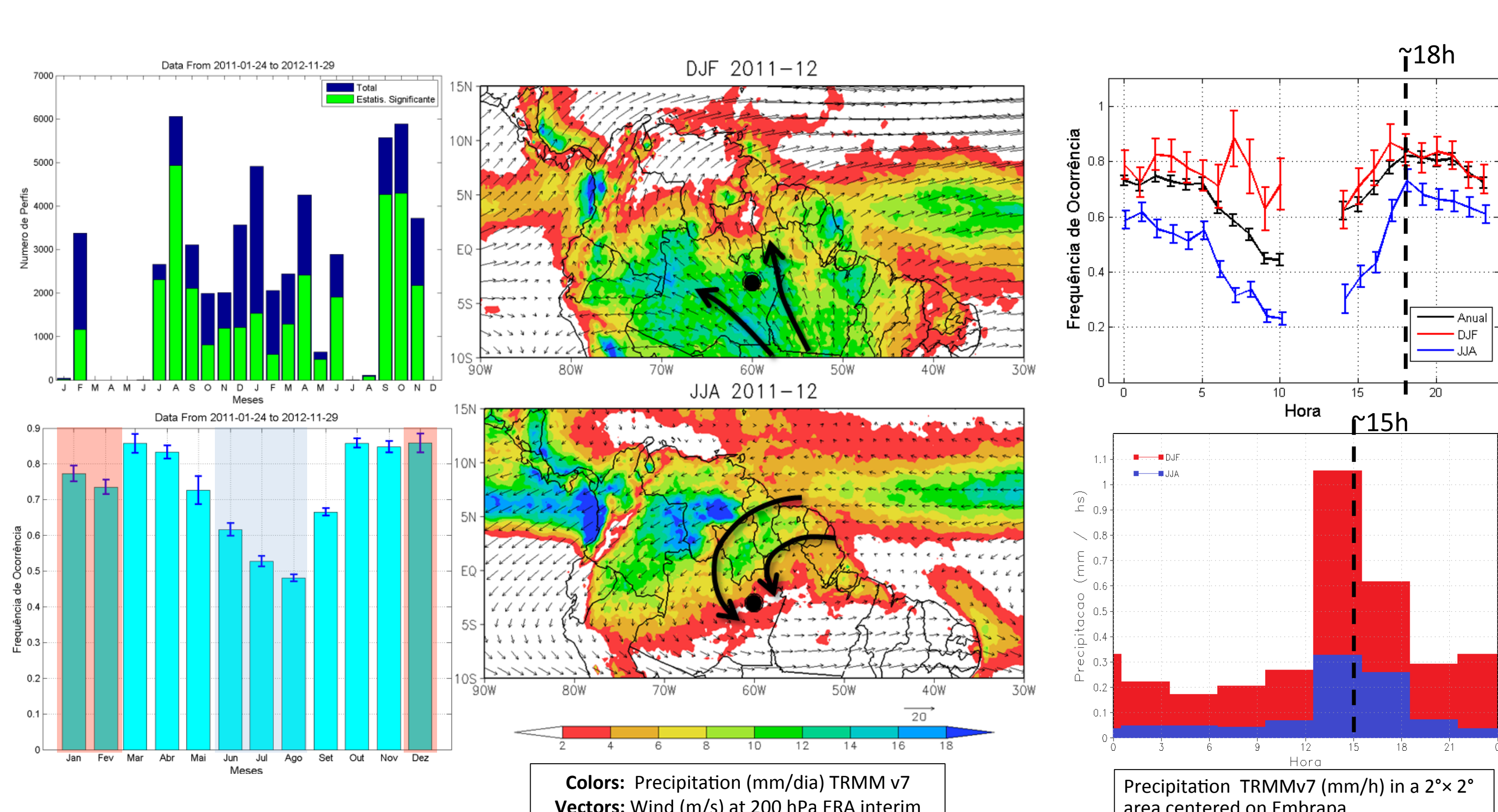
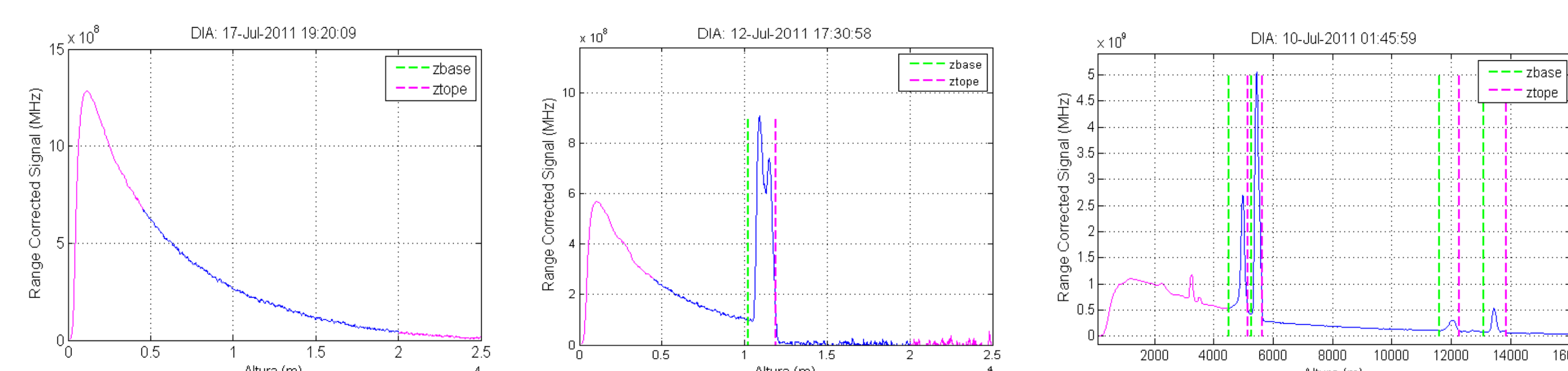
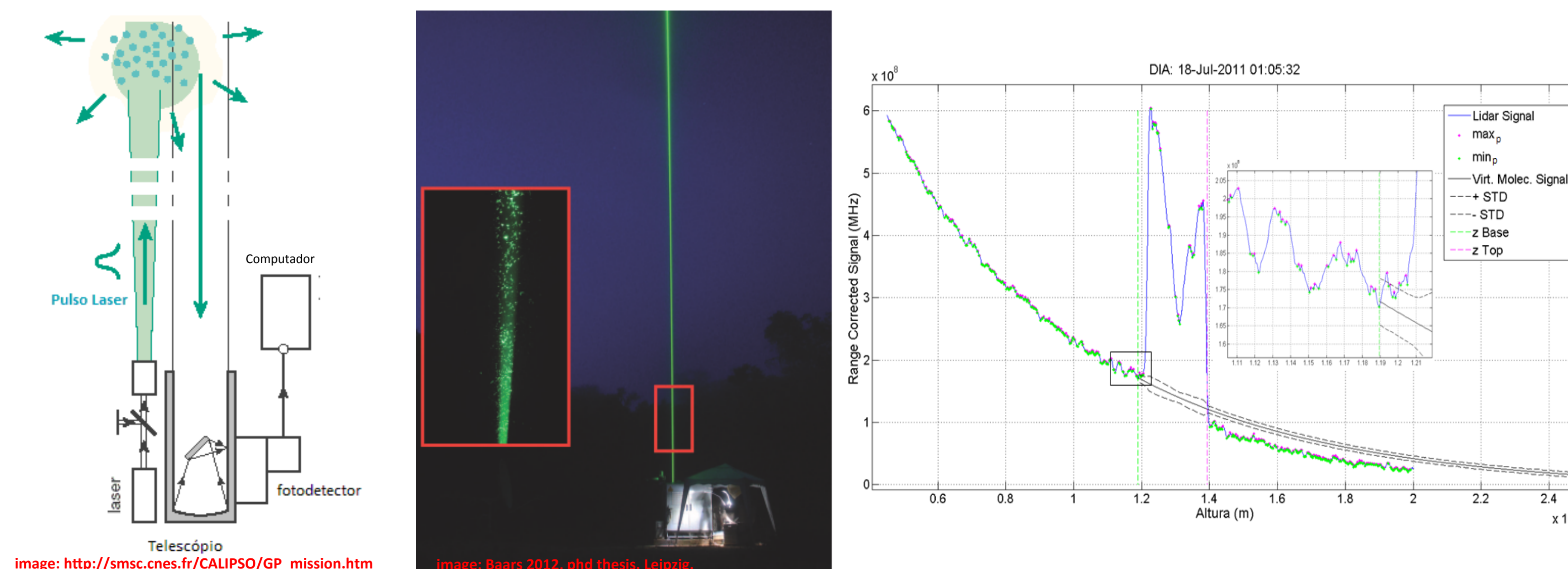


## ABSTRACT

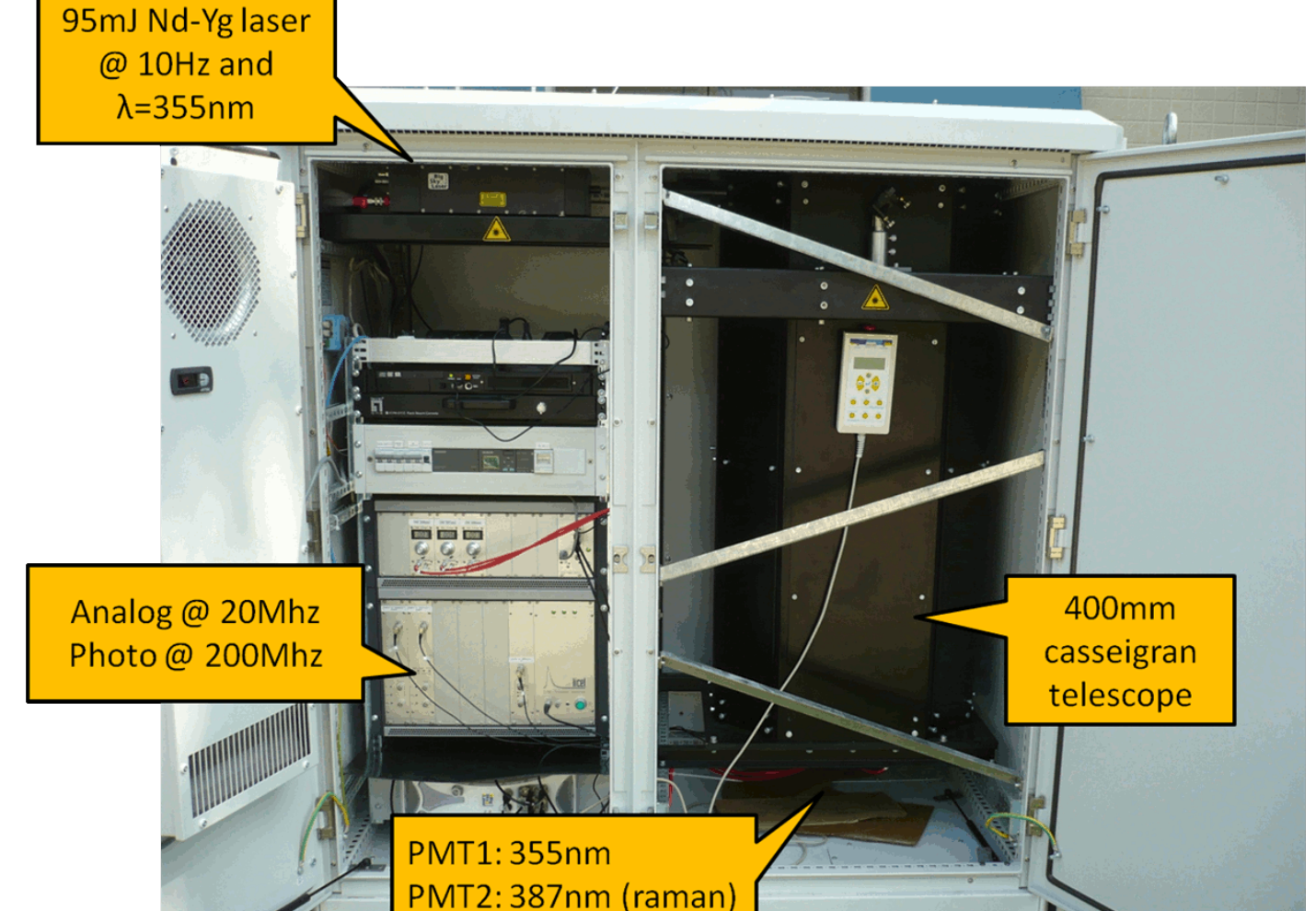
Cirrus clouds have been recognized as important agents of the climate system as they can significantly alter the radiation balance of the atmosphere. Despite being relatively transparent to solar radiation (optical depth < 3.0), they trap the infrared radiation that would be lost to space, and thus have a positive radiative forcing. They are found near the tropopause and are formed mainly by non-spherical ice crystals, with a lifetime that can go from hours to a few days. Its importance grows due to its large coverage area. The global cirrus cover has been estimated to be about 20-25% and their occurrence can be more than 70% over the tropics. In this paper, we report on tropical cirrus clouds characteristics as measured by a lidar station operational in the central Amazon region since 2011. An automated algorithm for the detection of cirrus clouds was developed, which is used to determine the clouds geometrical properties. The transmittance of the lidar signal was used to derive the cirrus optical depth. The Klett and Raman methods were used to derive the backscattering coefficient and to estimate the lidar-ratio of the cirrus clouds. As the results from the first two years of measurements (2011-2012), we found that the occurrence of cirrus clouds was approximately 71.0% of the total time of observation, and approximately 24.2% of all cirrus were subvisual ( $t < 0.03$ ), 40.7% were thin cirrus ( $0.03 < t < 0.3$ ) and 35.1% were cirrus stratus ( $t > 0.3$ ). The average values of the cirrus base and top altitudes were  $12.4 \pm 2.4$  km and  $14.3 \pm 2.2$  km, respectively, being found at temperatures down to  $-90^\circ\text{C}$  they reside most frequently near the tropopause. The lidar-ratio was estimated as  $20.0 \pm 6.8$  sr, indicating a mixed composition of thick plate and long column ice crystals. The behavior of these quantities with respect to temperature was studied. The diurnal cycle of the frequency and altitude, during both summer and winter, indicate anvil outflow to be the most important generation mechanism.



	Total	DJF	MAM	JJA	SON
Temporal Frequency of Occurrence [%]	71.0	78.1	82.8	52.0	77.3
Base Altitude [km]	12.5	12.5	12.6	12.6	12.4
std. dev.	2.4	2.7	2.5	2.1	2.3
Top Altitude [km]	14.3	14.1	14.4	14.1	14.4
std. dev.	2.2	2.4	2.2	1.8	2.3
Thickness [km]	1.82	1.61	1.87	1.52	2.00
std. dev.	1.53	1.30	1.62	1.30	1.63
Maximum Backscatter Altitude [km]	13.0	13.0	13.1	13.1	13.0
std. dev.	2.4	2.7	2.5	2.0	2.3
Temperature at Max. Backs. Altitude [° C]	-56.9	-56.8	-57.1	-57.5	-56.5
std. dev.	17.2	19.7	17.6	14.7	17.2
Lidar Ratio [sr]	20.0	18.6	19.0	21.5	19.8
std. dev.	6.8	6.5	6.5	7.7	6.2
Subvisual Cirrus [%]	24.2	25.0	21.4	37.9	18.9
Thin Cirrus [%]	40.7	34.4	38.0	43.6	42.1
Cirrus Stratus [%]	35.1	40.6	40.5	18.5	39.0

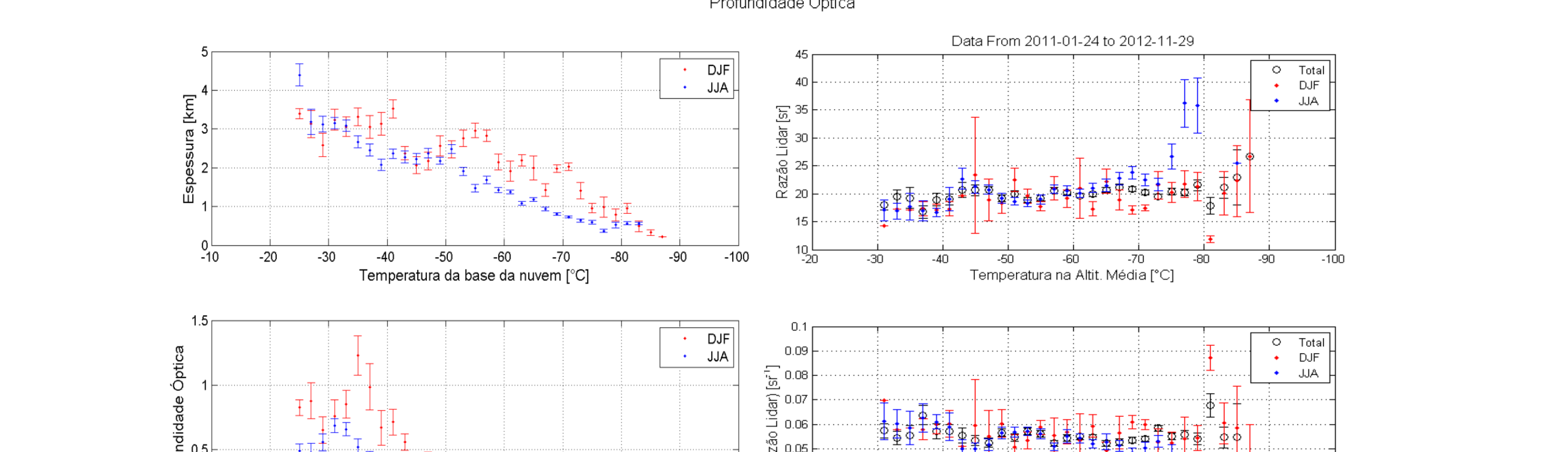
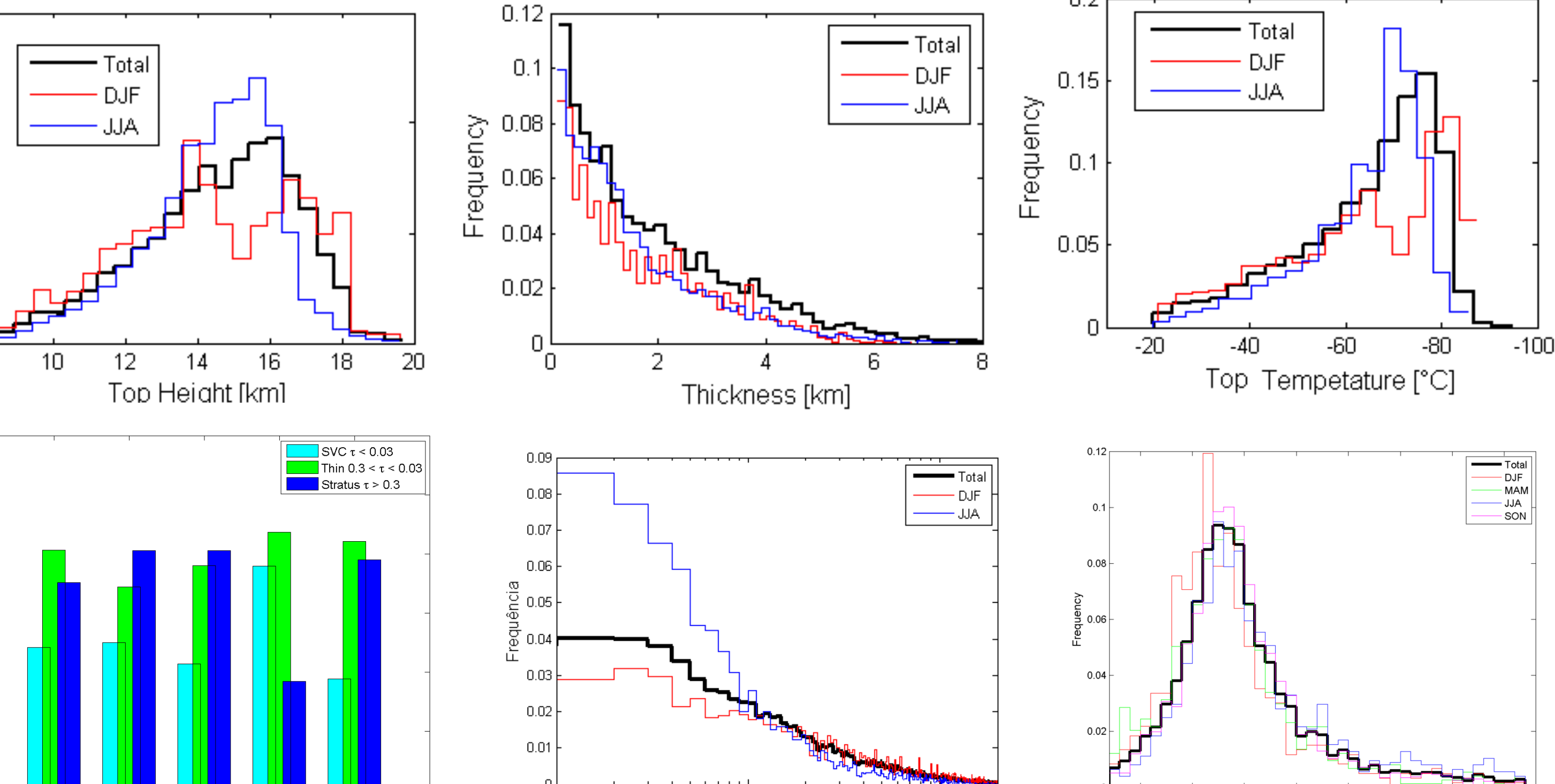
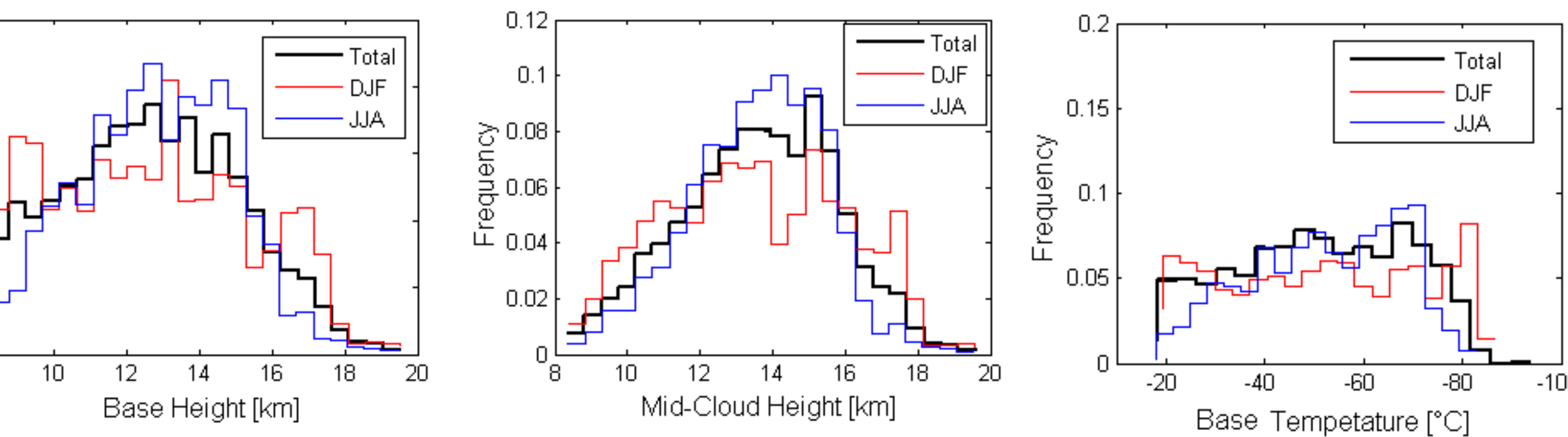
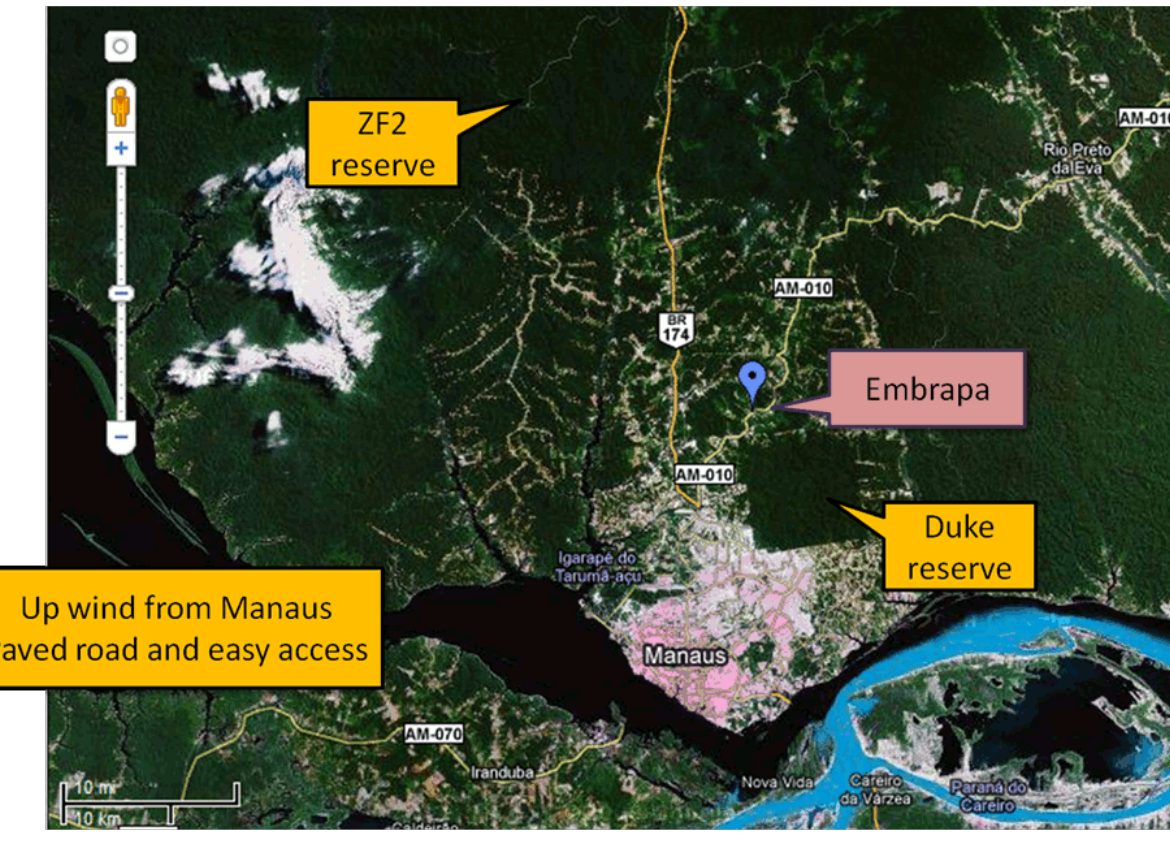
## OUR RAMAN LIDAR

Vertical resolution is 7.5m  
Range is 400m to 18km  
Derived quantities:  
**Back scatter coefficient**  
**extinction coefficient**  
**Water vapor**



95mJ Nd-Yg laser @ 10Hz  $\lambda=355\text{nm}$   
3 PMT's read 355nm (elastic), 387nm and 408nm (inelastic)  
Photon-counting @ 250 MHz  
Analog/Digital conversion @ 20 Mhz

## Embrapa Site – km30 AM-010



	Total	DJF	MAM	JJA	SON
Temporal Frequency of Occurrence [%]	71.0	78.1	82.8	52.0	77.3
Base Altitude [km]	12.5	12.5	12.6	12.6	12.4
std. dev.	2.4	2.7	2.5	2.1	2.3
Top Altitude [km]	14.3	14.1	14.4	14.1	14.4
std. dev.	2.2	2.4	2.2	1.8	2.3
Thickness [km]	1.82	1.61	1.87	1.52	2.00
std. dev.	1.53	1.30	1.62	1.30	1.63
Maximum Backscatter Altitude [km]	13.0	13.0	13.1	13.1	13.0
std. dev.	2.4	2.7	2.5	2.0	2.3
Temperature at Max. Backs. Altitude [° C]	-56.9	-56.8	-57.1	-57.5	-56.5
std. dev.	17.2	19.7	17.6	14.7	17.2
Lidar Ratio [sr]	20.0	18.6	19.0	21.5	19.8
std. dev.	6.8	6.5	6.5	7.7	6.2
Subvisual Cirrus [%]	24.2	25.0	21.4	37.9	18.9
Thin Cirrus [%]	40.7	34.4	38.0	43.6	42.1
Cirrus Stratus [%]	35.1	40.6	40.5	18.5	39.0

- [1] Goldfarb, L., Keckhut, P., Chanin, M.-L., and Hauchecorne, A.: Cirrus climatological results from lidar measurements at OHP (44°N, 6°E), Geophys. Res. Lett., 28, 1687–1690, 2001.  
[2] Hoareau, C., Keckhut, P., Noel, V., Chepfer, H., and Baray, J.-L.: A decadal cirrus clouds climatology from ground-based and spaceborne lidars above the south of France (43.9°N–5.7°E), Atmos. Chem. Phys., 13, 6951–6963, doi:10.5194/acp-13-6951-2013.  
[3] Larroza, E., Caracterização das Nuvens Cirrus nas Região Metropolitana de São Paulo (RMSP) com a Técnica de LIDAR de RETROESPALHAMENTO ELÁSTICO, Phd Thesis - IPEN (2011).  
[4] Barja, B., and Arocero, 2001. Cirrus Clouds at Camaguey, Cuba. Boris Barja and Roberto Arocero. Proceeding of the SPARC 2000.  
[5] Sassen, K., Z. Wang, and D. Liu : Cirrus clouds and deep convection in the tropics: Insights from CALIPSO and CloudSat, J. Geophys. Res., 114, D00H06, doi:10.1029/2009JD011916, 2009  
[6] Wang, Z. and Sassen, K. 2001: Cloud Type and Macrophysical Property Retrieval Using Multiple Remote Sensors. Journal of Applied Meteorology: Vol. 40, No. 10, pp. 1665–1682, 2001